

Synchrotron Powder Diffraction Study of Cements Pastes

E.O. Garcez^{1,2*}, L.P. Aldridge^{2,3}, M. Raven⁴, W.P. Gates², F. Collins², M. Franco⁵, F. Yokaichiya⁶

1) Universidade Federal de Pelotas- UFPel, Pelotas-RS, 96010-280, Brazil

2) Monash University, Department of Civil Engineering, Clayton – VIC, 3800, Australia;

3) Australian National Nuclear Research and Development Organisation-ANSTO, Lucas Heights-NSW, 2234, Australia;

4) Commonwealth Scientific and Industrial Research Organisation-CSIRO Land and Water, Urrbrae – SA, 5064, Australia;

5) Instituto de Pesquisas Energéticas e Nucleares- IPEN, 05508-000 - São Paulo, Brazil;

6) Helmholtz-Zentrum-Berlin für Materialien und Energie, Department Quantum Phenomena in Novel Materials, 14109 Berlin, Germany;

*Research fellow at Monash University with the Brazilian Science without Borders Program

Email: estelagarcez@gmail.com, laurie.aldridge@gmail.com

Available Online at: www.austceram.com/ACS-Journal

Abstract

Knowledge of the degree of hydration of cement pastes is critical for determining properties such as the durability of concrete. As part of an integrated study on the prediction of chloride ingress in reinforced concrete, synchrotron X-ray powder diffraction was used to estimate the degree of hydration of cement pastes. While for the past 20 years the composition of Portland cement has been determined by Rietveld analysis of X-ray diffraction, nevertheless there are a number of factors, including the amorphous content of the cement and relative proportion of mineral polymorphs present in the initial clinker, whose impact on the analysis are still not completely understood. Analysis of the resulting diffraction patterns indicated enhanced identification of polymorphs of alite, belite, ferrite and aluminate, which are present in the initial unhydrated cement and clinker, as well as improved quantification of hydrated crystalline phases such as calcium hydroxide and ettringite, which are key phases determining the speed of the chemical reactions in cement. In this paper we describe the experience that we have gained in the determination of the degree of hydration of cement pastes. We detail the standards and precautions that we took to characterize production cements and their hydration products.

Keywords: Innovation, Research, Cement and Concrete, Infrastructure, Durability.

INTRODUCTION

The degree of hydration of cement pastes underpins properties such as the durability of concrete. As part of an integrated study on the prediction of chloride ingress in reinforced concrete, synchrotron X-ray powder diffraction was used to estimate the degree of hydration of cement paste with and without supplementary cementitious materials such as fly ash and ground granulated blast furnace slag. In this preliminary report we compare Australian and Brazilian cements and determine the degree of hydration of selected pastes.

For Ordinary Portland Cement (OPC) and its pure components the degree of cement hydration by

quantitative X-ray diffraction analysis was determined by Copeland et. al (1960). Gutteridge (1984) used this technique to investigate the hydration of OPC fly-ash blend. Parrot and co-workers (1990) used quantitative x-ray diffraction analysis to establish correlations with indirect experimental methods of monitoring Portland cement hydration. Although X-ray diffraction remains one of the best and most powerful tools to measure the hydration rates of Portland cement, significant uncertainties remain that limit it being universally accepted. These uncertainties include the presence of amorphous as well as multiple crystalline phases in the cement and the formation of poorly crystalline phases during hydration that are not easily indexed by Rietveld methods.

In this work, Reitveld analysis was applied to synchrotron X-ray powder diffraction data to estimate the degree of hydration of cement pastes, as part of an integrated study on the prediction of chloride ingress in reinforced concrete, which is mainly focused on chloride transport in water saturated cement pastes.

At early ages the transport of water (and chloride ions) in cement paste is dependent on the existence of large interconnected pores – the so called capillary pores. When water is mixed with the cement powder (sized between ~1,000-40,000 nm) the water can be envisaged to form a continuous pore structure, which as the cement hydrates, becomes closed by hydration products formed. Thus, because the degree of hydration defines the amount of closure of this continuous pore structure, it can be described as a critical variable in controlling the retardation of chloride transmission. The influence of supplementary material in blended cements will be also investigated in the future.

METHODS AND PROCEDURES

X-ray diffraction patterns from Australian and Brazilian Cements were run at both the Australian and Brazilian Synchrotrons. Clinker and cement CPV - high early strength Portland cement (ABNT NBR 5733:1991) from Brazil were used in this study. This cement is the only commercial cement in Brazil which has no supplementary materials such as pozzolan or granulated blast furnace slag added to its composition. Ordinary Portland Cement (OPC) from Australia was also used.

Sample preparation

For CPV, diffraction patterns of clinker, cement powder and cement pastes aged from 1 hour curing up to 28 days (672 hours) were measured using the X-ray powder diffraction beamline at LNLS. Diamond powder (MONO-ECO monocrystalline diamond, particle size 0-1 μm , sourced from Microdiamant AG) was chosen as an internal standard in a content of 10 wt% (or 0.1g of diamond per 0.9g of sample).

Clinker was hand ground to a very fine powder and measured with and without diamond powder. Cement powder was measured 'as received' (not ground) with 10% of diamond powder admixed. The powder mixtures were carefully placed in the front mounted sample holder (flat plate) in order to minimize sample orientation. For the hydration measurements, several samples were prepared, and measurements from 1 to 24 hours were collected with a cement paste ($a/c=0.42$) prepared at the LNLS facilities, following the ABNT NBR 7215:1996 procedure. A content of 10% of diamond powder was added in the mixture. The paste was placed in the sample holder and

covered with Kapton® tape. Measurements started one hour after sample casting. For the measurements from 168 to 672 hours (7 to 28 days), pastes ($a/c=0.42$) were prepared in advance in a concrete lab to allow the samples to age. Pastes were mixed and placed in cylindrical moulds. Immediately after casting, cylinders were placed in plastic bags with wet paper towel. After 24 hours, samples were demoulded and cured inside plastic bags with wet towel until measurements. At the LNLS facilities, samples were dried at 65°C in a convection oven to drive off water to a moisture content variation (mass %) lower than 1%. Dried pastes were then hand ground and mixed with 10% diamond powder prior to packing into the sample holder for X-ray analysis.

For OPC samples, cement pastes ($w/c=0.42$) having curing times of 1, 3, 5, 7, 14 and 28 days were studied. For these experiments, pastes were hand ground and loaded in 0.5 mm glass capillaries (CTS Capillary Tube Supplies Ltd, UK). Samples containing an internal standard were doped with 10 wt% corundum powder prior to loading. Samples of pure unhydrated OPC with and without corundum were also measured.

Beamlines

The experiments with Brazilian cement (CPV) were performed at the X-ray powder diffraction beamline D10B-XPD [1], at the Brazilian Synchrotron Light laboratory (LNLS). The X-ray diffraction data were obtained using 4+2-circle Huber diffractometers and a Mythen detector [2]. The sagittal double crystal monochromator Si (111) was used to provide a monochromatised beam of 9 keV (1.3769 Å). This configuration was chosen in order to minimize the superposition of neighboring Bragg peaks. Data were obtained at room temperature, in a θ - 2θ geometry (Bragg-Bretano configuration), with a flat plane sample holder, over a 2θ range of 10°-50° with a step size of 0.005° and exposure time of 1s. During measurements samples were spined around the vertical axis to improve particle statistics.

The Australian OPC was measured at the Australian Synchrotron powder diffraction beamline set up at 15 keV (0.082 nm) radiation, and measured over two angular ranges with the solid-state detector and data normalised using PDViPer software provided by the Australian Synchrotron Powder Diffraction Beamline team.

RESULTS AND DISCUSSION

Phase identification and Rietveld quantitative phase analysis were carried out using Topas-Academic v.5. A background polynomial of 3 coefficients was used.

Preferred orientation corrections were applied when necessary.

Phase Identification

A few assumptions following Taylor (1997) were necessarily made to permit phase identification of the clinker:

1. C_3S (alite) in cement clinker generally exists in the monoclinic, triclinic or rhombohedral forms;
2. C_2S (belite) in clinker generally exists only in the beta polymorph;
3. The C_3A (aluminite) clinker is generally either in the cubic or orthorhombic forms;
4. The C_4AF (ferrite) in typical cement clinkers approximates to $Ca_2AlFe_{0.6}Si_{0.16}Ti_{0.05}O_5$ ($CaAl_{1.4}Fe_{0.6}O_5$) (Redhammer et al.).

Miller & Tang (1996) observed, from analysis of 33 European and North American clinkers, that in addition to the sulphates incorporated into the clinker (principally in the belite phase) the following sulphates were present: arcanite (K_2SO_4), apthitalite (a solid solution series nominally $3K_2SO_4 Na_2SO_4$), and calcium langbeinite (usually designated $2CaSO_4 - K_2SO_4$). Also Cruz et. al (1986) claim that calcium langbeinite and arconite can be found in Spanish clinker. Furthermore when the clinker was exposed to water syngenite formed.

In the Brazilian clinker and cement (CPV) only the triclinic form of C_3S was identified; C_3A was better represented by the orthorhombic form; C_4AF , described as $Ca_2(Fe_{2-x}Al_x)O_5$, was better represented with $x=1.0$ rather than $x=1.4$; while arcanite (K_2SO_4) was observed, both apthitalite ($3K_2SO_4 Na_2SO_4$) and Ca-langbeinite ($2CaSO_4 - K_2SO_4$) were not present.

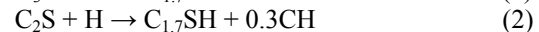
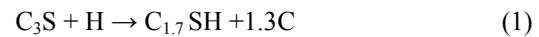
In hydrated cement, the limited amount of arcanite (K_2SO_4) present in CPV appeared to dissolve in the first hour of hydration. It is important to note that arcanite and C_3S triclinic have peaks at approximately $2\theta = 26.2^\circ$, consequently arcanite might be underestimated. Calcite was present and disappeared after 7 hours of hydration. At this stage, Portlandite appeared and increased subsequently. Bassanite, which is present in cement, disappeared as soon as the hydration process started.

For the Australian Cement (OPC) all three forms of the C_3S – monoclinic, triclinic and rhombohedral – were found. C_3A was present in cubic form. C_4AF was also better fit with $x=1.0$ in $Ca_2(Fe_{2-x}Al_x)O_5$. Gypsum, bassanite and calcite were present. Periclase, arcanite, Ca-langbeinite and syngenite were present but apthitalite was not. Anhydrite, quartz and calcium oxide (CaO) were not observed.

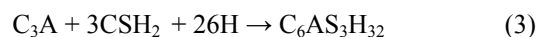
Phase quantification

According to Taylor (1990), during the middle period of hydration, starting at about 3h and ending at about 24 hours, some 30% of the cement reacts and it is best characterized by the formation of calcium hydroxide (CH) as well as nearly amorphous calcium silicate hydroxide (CSH) crystals. At 28 days, 70% of C_3S typically reacts. For CPV, which is high early strength cement, it can be observed that approximately 50% of alite (C_3S) has reacted within the first 24 hours of hydration. Most of the subsequent reaction occurred during the first few days, which may lead to substantial strength gains and reduction in capillary porosity. After 28 days (672 hours), only about 15% of the initial C_3S was unreacted.

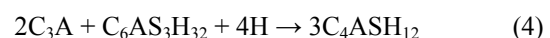
The C_2S (belite) hydration products are the same as those of C_3S , but the relative amount of CH formed is less, as seen in Eqn 1 and 2.



C_2S is much less soluble than C_3S , so the rate of hydration was much slower, contributing little to the early strength of cement. As C_3S reacted, the diffraction pattern showed that Portlandite (CH) and amorphous content both increased, mainly after 9 hours of hydration. The growth of amorphous content characterizes the formation of both amorphous or very poorly crystalline CSH phase. Tricalcium aluminate (C_3A) is highly soluble. In the presence of gypsum (CSH_2), which prevents the rapid hydration of C_3A , ettringite ($C_6AS_3H_{32}$) is formed accordingly to Eqn 3:



If the gypsum in the cement reacts completely before the C_3A , the concentration of sulphate ions in the pore solution decreases drastically and the ettringite becomes unstable and converts to a different solid phase with less sulphate, called monosulfoaluminate Afm (C_4ASH_{12})



For CPV, the quantification of C_3S , C_3A , C_2S and C_4AF phases from 1 to 672 hours of hydration can be observed in Fig. 1 and 2. As shown in Fig. 3, gypsum was no longer detectable after 10 hours of hydration. Ettringite was not detected in the first hours and only appeared in small amounts in the 7 days (168 hours) aged sample. The presence of AFm became more evident after 14 days of hydration. It is important to note that accordingly to equation 3 and also as stated by Taylor (1990), ettringite should be detectable in

cements at ordinary temperatures within a few hours and increase in proportion to a maximum, often at about 24 hours. At this stage, the conversion reactions (e.g. Equation 4) lead to the dissolution of ettringite and precipitation of monosulfate. Monosulfate is also poorly crystalline and its diffraction maxima may be observed only after some days or even months. However, for cements of relatively high SO_3/Al_2O_3 ratios, not all the ettringite may disappear and monosulfate may not be detected. With sulphate resisting Portland cement, in which the amount of C_3A is restricted to lower than 5 % and $(2 C_3A + C_4AF)$ is lower than 25%, ettringite persists for periods of up to 1 year. No ettringite peaks were detected for CPV in the first 24 hours, but the existence of ettringite in longer aged samples, indicates that CPV may be a sulphate resistant cement type.

The ferrite phase (C_4AF), as expected, reacted slower than C_3A , as seen by their curves in Fig. 2, and the hydration products of phases were essentially similar to those formed from C_3A , i.e., ettringite and monosulfate. Monosulphates are quantified as amorphous material in the diffraction patterns due to their poorly crystalline characteristics and its growth can be seen in Fig. 4. The Rietveld refinement of CPV sample hydrated for 24 hours is shown in Fig 15 at the end of this paper.

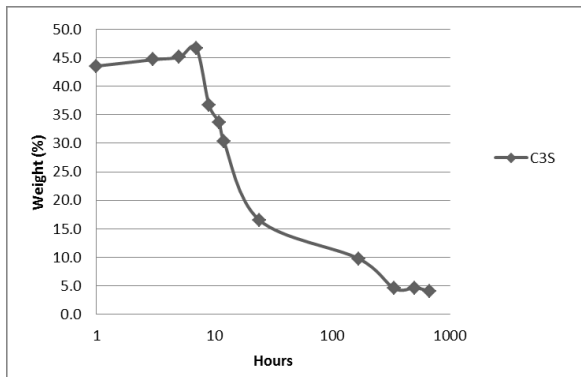


Fig. 1: Alite (C_3S) quantification for CPV

For the Australian OPC, C_3S in triclinic, monoclinic and rhombohedral forms were present for unhydrated OPC and for OPC pastes hydrated from 24 to 672 hours (1 to 28 days). The content of each polymorph can be seen in Fig. 5. The content of belite (C_2S), aluminat (C_3A) and ferrite (C_4AF) of hydrated OPC pastes can be seen in Fig. 6. Gypsum, bassanite, anhydrite, ettringite and calcite content are shown in

Fig. 7. Ettringite was observed after 24 hours curing and its content tended to decrease with aging. The development of Portlandite and amorphous content of OPC is shown in the Fig. 8.

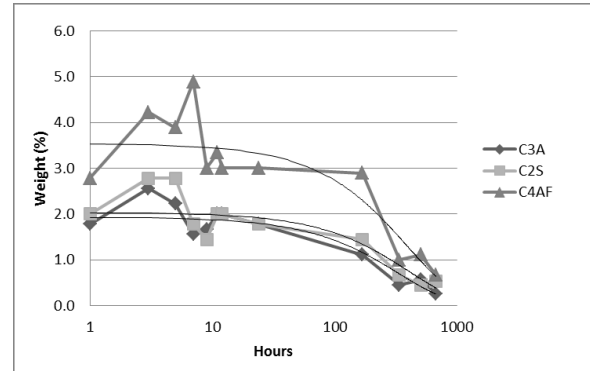


Fig. 2: Aluminat (C_3A), Belite (C_2S) and Ferrite (C_4AF) quantification for CPV

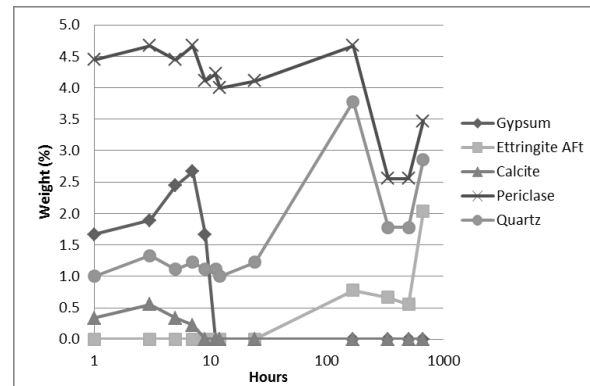


Fig. 3: Gypsum, Ettringite, Calcite, Periclase and Quartz quantification for CPV

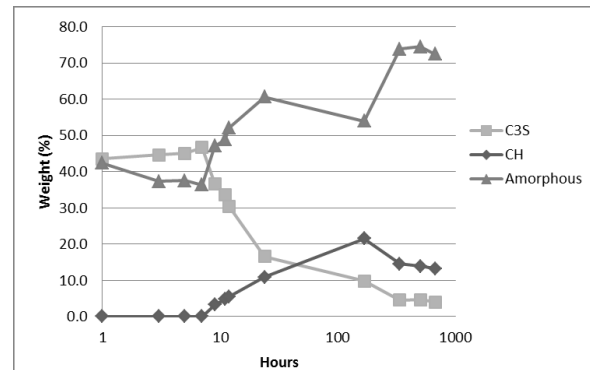


Fig. 4: C_3S versus Portlandite (CH) and amorphous content of CPV

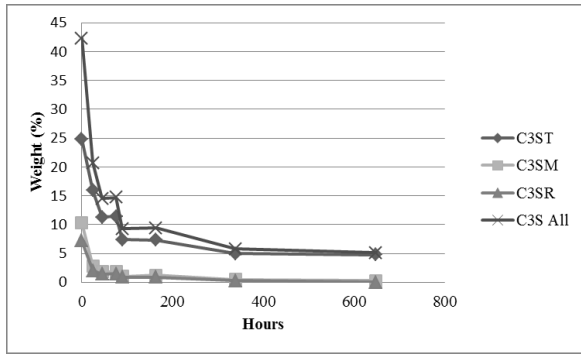


Fig. 5: Alite (C₃S) polymorphs quantification

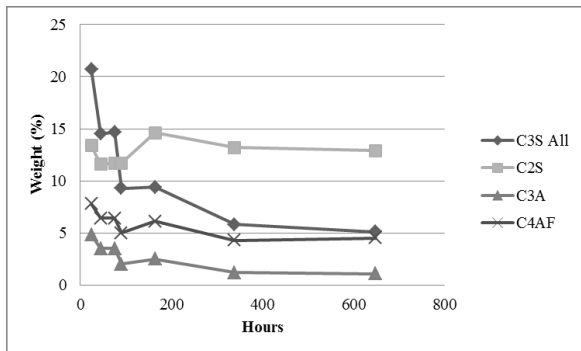


Fig. 6: Alite (C₃S), Belite (C₂S), Aluminate (C₃A) and Ferrite (C₄AF) quantification for OPC pastes hydrated from 24 to 672 hours (1 to 28 days)

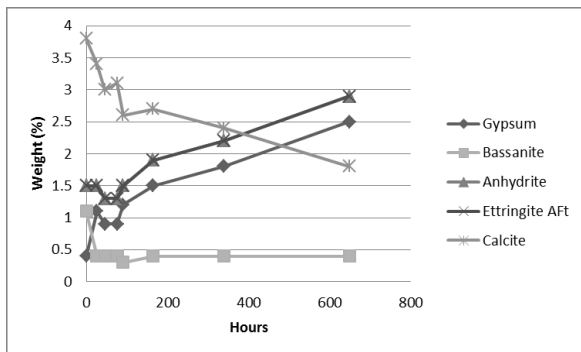


Fig. 7: Gypsum, Bassanite, Anhydrite, Ettringite and Calcite quantification for OPC

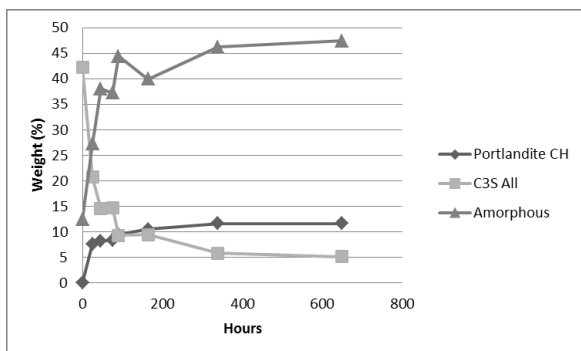


Fig. 9: C₃S, CH and amorphous content of OPC

The comparison between CPV and OPC contents of C₃S, C₂S and C₃A are shown in Fig. 10 to 12. The hydration of C₃S was very similar for both cements. C₃A in CPV reacted more during the first 24 hours than OPC. CPV had lower weight percentage of C₂S when compared to OPC, which would impact the hydration rate as observed.

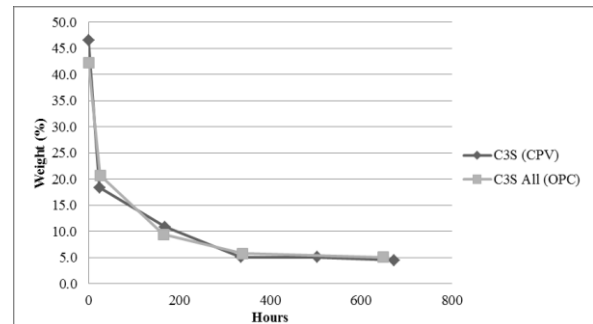


Fig. 10: C₃S content of CPV and OPC from 24 to 672 hours of hydration

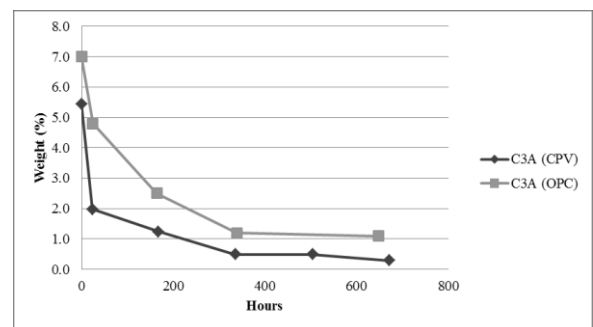


Fig. 11: C₃A content of CPV and OPC from 24 to 672 hours of hydration

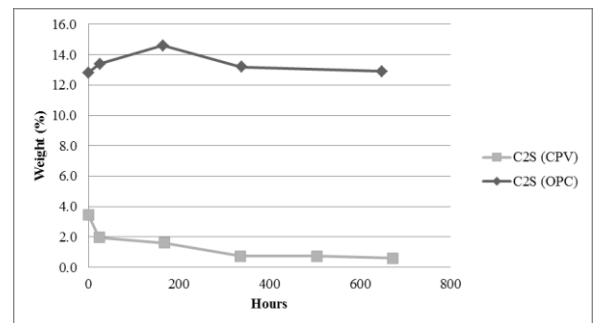


Fig. 12: C₂S content of CPV and OPC from 24 to 672 hours of hydration

Degree of hydration

The kinetics of cement hydration is related to the relations between the degree of hydration (α) and the age (t), and the factors that influence them. From a practical standpoint, the kinetic curve controls the way in which the physical properties, such as durability, develop as curing proceeds. α may relate either to an individual clinker phase or to the cement as a whole. Because cement is a mixture of phases

that react at different rates, there are significant problems in determining, and even in defining, α for the whole cement (Taylor, 1990) Parrot et. al (1990) described the degree of hydration of a polyphase material such as cement by:

$$\alpha = \sum_{i=1}^{i=n} f_i \alpha_i$$

Where α_i is the degree of hydration of phase i and f_i is the original weight fraction of phase i . The direct determination of the degree of hydration of a single or polyphase material may be performed by measuring the fraction of unreacted phase i , x_i , giving

$$\alpha_i = 1 - x_i$$

The degree of hydration of CPV and OPC monitored by quantitative X-Ray diffraction analysis at different curing ages is illustrated in Fig. 13. CPV is designed to reach the same strength in the first 7 days of hydration as OPC aged 28 days. Thus, it was expected that a higher rate of hydration in the first days of aging would be observed, followed by retardation of hydration speed, particularly after 7 days. As shown in the Fig. 13, the CPV sample investigated in this work shows a quick development in hydration between 9 and 24 hours, reaching a degree of hydration about 0.6. After this stage, the

hydration reactions slow, and reach a degree of hydration of approximately 0.9 at 28 days.

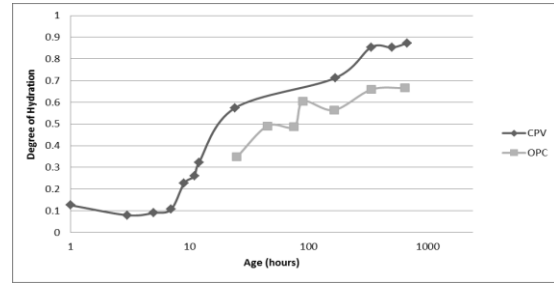


Fig. 13: Degree of hydration of CPV and OPC in logarithmic scale

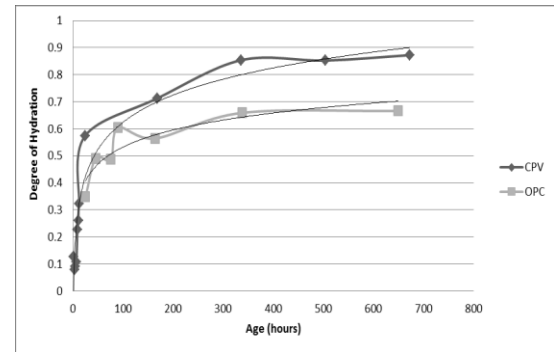


Fig. 14: Degree of hydration of CPV and OPC in normal scale

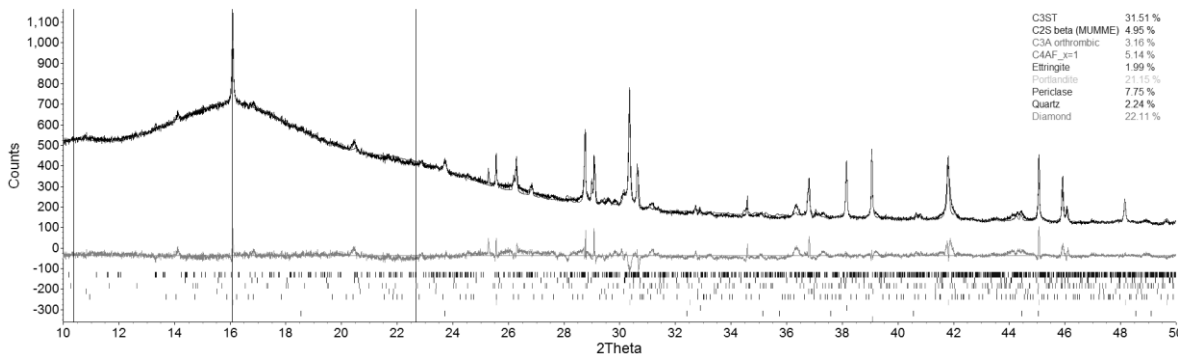


Fig. 15: X-ray diffraction pattern of CPV aged 24 hours

CPV has higher degree of hydration at all ages when compared to OPC. Fig. 14 shows that up to 168 hours, CPV hydration rate was higher than OPC, due to its fineness, probably in combination with the absence of sulphates. Furthermore, OPC had a much greater C_2S/C_3S ratio when compared to CPV, which would be expected to retard the hydration rate. After 168 hours, the hydration develops nearly in the same rate.

CONCLUSIONS

The use of synchrotron radiation allowed us to continuously monitor hydration reactions of cements

and compare the hydration from two production cements over 1 to 672 hours.

Topas-Academic v.5 proved to be a powerful tool to apply Rietveld analysis on the cement pastes. However, the analyses are very sensitive to errors introduced by the presence of different polymorphic forms of cement phases, errors in crystal structures, and errors in the input file parameters, which may be deceptive and difficult to correct, but will produce unrealistic results. A substantial knowledge on cement chemistry is essential to produce acceptable Rietveld analysis.

One of the differences between both cements is the existence of all three C_3S polymorphs in the Australian cement, while the Brazilian only presents the triclinic form. However, the major difference with regards to hydration is due to the different C_2S contents. C_2S has a lower hydration rate when compared to the other cement phases and also contributes little to early strength. CPV has very limited content of C_2S , and thus presented a higher degree of hydration at all investigated ages, as expected for high early strength cement. The results presented in this paper will be further related to pore size and pore distribution, and used to quantify the influence of porosity on chloride ingress into concrete. The influence of supplementary material in blended cements will be also investigated.

ACKNOWLEDGMENTS

The authors would like to acknowledge the Science without Borders Program, from *Conselho Nacional de Desenvolvimento Científico e Tecnológico (CNPq)* of the Ministry of Science, Technology and Innovation of Brazil, The Brazilian Synchrotron Light Laboratory (LNLS), The Australian Synchrotron and The Australian Research Council's Discovery Research Program for funding (DP120102203).

REFERENCES

1. **F. F. Ferreira, E. Granado, W. Carvalho, S. W. Kycia and R. Droppa**, X-ray powder diffraction beamline at D10B of LNLS: application to the Ba_2FeReO_6 double perovskite, *Journal of Synchrotron Radiation*, 13 (2006) 46-53.
2. **A. Bergamaschi, A. Cervellino, R. Dinapoli, F. Gozzo, B. Henrich, I. Johnson, P. Kraft, A. Mozzanica, B. Schmitt and X. Shi**, The MYTHEN detector for X-ray powder diffraction experiments at the Swiss Light Source, *Journal of Synchrotron Radiation*, 17 (2010) 653-668.
3. ABNT NBR 7215:1996: Portland cement - Determination of compressive strength (in Portuguese).
4. **G. J. Redhammer, G. Tippelt, G. Roth and G. Amthauer**. Structural variations in the brownmillerite series $Ca_2(Fe_{2-x}Al_x)O_5$. Sample: bht120n2, *American Mineralogist*, 89 (2004) 405-420.
5. **J.C. Madsen and N.V.Y. Scarlett**, Cement: Quantitative Phase Analysis of Portland Cement Clinker, *Industrial Applications of X-Ray Diffraction*
6. **F.M. Miller and F.J. Tang**, The Distribution of Sulfur in Present-Day Clinkers of Variable Sulfur Content. *Cement and Concrete Research*, [26], 12, (1996) 1821-1829
7. **I. de la Cruz, T. Vázquez, and O.F. Peña**, IR spectroscopy of sulphates in clinkers and cement. *Materiales de Construcción*, [36], 201, (1986) 25-42.
8. **E. Corazza and C. Sabelli**, The crystal structure of syngenite, $K_2Ca(SO_4)_2 \cdot (H_2O)$ Locality: Kalasz, Galicia, *Zeitschrift für Kristallographie*, [124], (1967) 398-408.
9. **I.V. Pekov, M.E. Zelenski, N.V. Zubkova, V.O. Yapaskurt, N.V. Chukanov, D.I. Belakovskiy, and D.Y. Pushcharovsky**, $K_2Ca_2(SO_4)_3$, a new mineral from the Tolbachik volcano, Kamchatka, Russia, *Mineralogical Magazine*, [76], (2012)
10. **D. Speer and E. Salje**, Phase transitions in langbeinites I: Crystal chemistry and structures of K-double sulfates of the langbeinite type $M_{2++}K_2(SO_4)_3$, $M_{++} = Mg, Ni, Co, Zn, Ca$. *Physics and Chemistry of Minerals*, [13], (1986) 17-24.
11. **L. J. Parrot, M. Geiker, W. Gutteridge and D. Killoh**. Monitoring Portland Cement Hydration: Comparison of Methods. *Cement and Concrete Research*, 20:919-926 (1990)
12. **R. Snellings, A. Bazzoni and K. Scrivener**. The existence of amorphous phase in Portland cements: Physical factors affecting Rietveld quantitative phase analysis, *Cement and Concrete Research* 59:139-146 (2014)
13. **P.M. Suherman, A. Riessen, B. O'Connor, D. Li, D. Bolton and H. Fairhurst**. Determination of amorphous phase levels in Portland cement clinker Powder Diffraction 17 (2002)
14. **P.S. Whitfield and L.D. Mitchell** (2003) Quantitative Rietveld analysis of the amorphous content in cements and clinkers, *Journal of Materials Science* 38:4415-4421
15. **D. Jansen, C. Stabler, F. Goetz-Neunhoffer, S. Dittrich and J. Neubauer**, (2011) Does Ordinary Portland Cement contain amorphous phase? A quantitative study using an external standard method, *Powder Diffraction* 26:31-38
16. **L. E. Copeland and R. H. Bragg**, Quantitative X-Ray Diffraction Analysis, *Anal. Chem*, 30:196-201 (1958)
17. **W. Gutteridge**, Quantitative X-Ray Powder Diffraction in the Study of Some Cementive Materials, *Brit. Ceram. Proc. No.* 35:7-15 (1984)